A molecular dynamics investigation of fluorocarbon based layer-by-layer etching of silicon and SiO_2 ⊘

S. Rauf; T. Sparks; P. L. G. Ventzek; V. V. Smirnov; A. V. Stengach; K. G. Gaynullin; V. A. Pavlovsky

Check for updates

View Online

Export Citation

A molecular dynamics investigation of fluorocarbon based layer-by-layer etching of silicon and SiO$_2$

S. Rauf,[a)] T. Sparks, and P. L. G. Ventzek
Freescale Semiconductor, Inc., 3501 Ed Bluestein Bonlevard, MD K-10, Austin, Texas 78721

V. V. Smirnov, A. V. Stengach, K. G. Gaynullin, and V. A. Pavlovsky[b)]
SarovLabs, Sarov, Russia

A molecular dynamics model is used to understand the layer-by-layer etching of Si and SiO$_2$ using fluorocarbon and Ar$^+$ ions. In these two-step etch processes, a nanometer-scale fluorocarbon passivation layer is grown on the material's surface using low energy CF$_x^+$ ions or radicals. The top layers of the material are then reactive ion etched by Ar$^+$ ions utilizing the fluorocarbon already present on the material surface. By repeating these two steps, Si or SiO$_2$ can be etched with nanometer-scale precision and the etch rate is considerably faster than what traditional atomic layer etching techniques provide. The modeling results show that fluorocarbon passivation films can be grown in a self-limiting manner on both Si and SiO$_2$ using low energy CF$_2^+$ and CF$_3^+$ ions. The fluorocarbon passivation layer is a few angstroms thick, and its thickness increases with the fluorocarbon ion's energy. Increasing the ion energy, however, amorphizes the top atomic layers of the material. In addition, the fluorocarbon film becomes F rich with increasing ion energy. Simulations of fluorocarbon passivated SiO$_2$ surface show that Ar$^+$ ions with energy below 50 eV etch Si (within SiO$_2$) in a self-limiting manner. Si etching stops once F in the fluorocarbon passivation layer is exhausted or is pushed too deep into the substrate. Oxygen within SiO$_2$ is more easily sputtered from the material surface than Si, and the top layers of SiO$_2$ are expected to become O deficient during Ar$^+$ ion bombardment. Ar$^+$ ion etching of fluorocarbon passivated Si also appears to be self-limiting below 30 eV ion energy, and etching stops once F on the material surface is either consumed or becomes inaccessible. © *2007 American Institute of Physics*.
[DOI: 10.1063/1.2464192]

I. INTRODUCTION

Microelectronic device dimensions are rapidly shrinking and subnanometer control of device dimensions is expected to become essential in the near future. Many techniques have been developed to enable dimensional control with such high degree of precision. These techniques include atomic layer deposition[1–3] (ALD) and atomic layer etching (ALE).[4–20] Both techniques are pulsed in nature and make use of self-limiting growth processes in which deposition is limited to a few angstroms during each step. During ALD, several such self-limiting deposition processes are alternated to deposit films in a layer-by-layer fashion. In many ALE schemes, following the deposition of a subnanometer thick passivant, the top monolayer or less of the substrate is removed using energetic ions,[5] ultraviolet radiation,[6] or through thermal means.[7] ALD has found many applications in microelectronics including the deposition of high-κ gate dielectrics[1] and metallic diffusion barriers for copper interconnects.[2] However, ALE is still not widely used, one of the primary hindrances being its extremely slow etch rate. ALE etch rates are slow enough that the use of ALE for the fabrication of microelectronics devices is currently economically impractical. Current plasma etching techniques, on the other hand, do

not allow the degree of control necessary for fabricating devices with subnanometer precision. There is therefore a need for etching processes that proceed at a reasonable rate, but allow subnanometer-scale control of film dimensions. One potential solution for such an etch process is to use a pulsed technique similar to ALE but etch several monolayers during each cycle. This can be achieved, for example, through the deposition of nanometer-scale fluorocarbon passivation layers. Previous experimental work has shown that such passivation films can be grown using fluorocarbon plasmas, ions, or radicals.[21–28] Our article attempts to elucidate the details of such pulsed etching processes for Si and SiO$_2$. A molecular dynamics (MD) model is used for this purpose, and the model is used to examine both the deposition and etching steps during the layer-by-layer etching of Si and SiO$_2$.

Our investigation builds on insight from experiments in recent years that have started to shed light on the fundamental mechanisms responsible for the etching of Si and dielectrics (e.g., SiO$_2$ and Si$_3$N$_4$).[21–26] According to the qualitative picture that has emerged from this work, a nanometer-scale fluorocarbon reactive layer forms on the material surface when it is exposed to a fluorocarbon based plasma. Both low energy ions and neutral fluorocarbon radicals are known to contribute to the growth of this fluorocarbon (CF) polymer film.[27,28] When energetic ions bombard the CF-polymerized Si or dielectric surface, they are able to etch the underlying material at a rate substantially faster than possible through

a)Electronic mail: rauf@ieee.org
b)Electronic mail: vladimir.pavlovsky@sarovlabs.com

physical sputtering alone. The radical and ion compositions of the plasma determine CF-polymer properties, which in turn impacts ion etching characteristics. Experimental work has also characterized the fundamentals of spontaneous etching processes, one monolayer at a time.[29–31]

MD has been used to investigate ion etching in many related systems in the past. Abrams and Graves[32–35] developed a MD based model for an etch system comprising of Si, C, and F and used this model to investigate Si etching using CF_x^+ ($x=0-3$) ions. Their modeling results indicated that a reactive layer forms on the Si surface, and the structure of this SiC_xF_y reactive layer is more complicated than etching with only F or Cl. The thickness of the reactive layer increased with the energy of the bombarding radical. Abrams and Graves characterized etch byproduct distributions as a function of ion energy, looked at the differences between etching due to the different CF_x^+ ($x=0-3$) ions, and attempted to capture their complex MD results in terms of a simple set of mass balance equations. Ohta and Hamaguchi[36] developed pseudopotentials for Si–O–F and Si–O–Cl etch systems and used them in MD simulations to investigate the sputtering of SiO_2 by F^+, Cl^+, and Ar^+ ions. It was found that F^+ and Cl^+ are more reactive compared to Ar^+ ions, resulting in higher etch yields for comparable energies. Smirnov *et al.* have recently investigated the fluorocarbon ion etching properties of SiO_2.[37,38] Detailed analysis of sputtered clusters has shed light on energy and angular distribution of various etched clusters and surface etching reactions. Athavale and Economou[4] used MD to investigate ALE of Si using Cl^+ and Ar^+ ions.

This article is organized in the following manner. Our computational model is described in Sec. II, and computational results are discussed in Sec. III Concluding remarks are in Sec. IV.

II. COMPUTATIONAL MODEL

The computational model used in the present study has been described in detail in Ref. 37. We therefore only briefly discuss the model's key features in this article. Simulations have been conducted using a MD based model that can take account of interactions between Si, O, C, and F. In the model, pseudopotentials for two- and three-body interactions have either been obtained from the literature or computed using *ab initio* techniques utilizing GAUSSIAN98.[39] The Stillinger-Weber potential construct has been used to represent pseudopotentials, and velocity-Verlet algorithm[40] is used to advance particle trajectories. Following ion impact, material temperature is controlled using the Berendsen thermal bath model.[41] In the primary computational experiments reported in this article, energetic fluorocarbon (CF_2^+, CF_3^+) or Ar^+ ions are bombarded on modeled surfaces and characteristics of material ejected from the surface or deposited on the surface are analyzed.

Several aspects of this model have been validated against available data.[37] This includes the validation of the underlying pseudopotentials by comparing computed binding energies and bond lengths with experiments and other theoretical work. Results are presented in Ref. 37 and the agreement between our calculations and previously available data is considered reasonable. The overall computational model and the modeled SiO_2 surface are validated by comparing the computed sputter yield for Ar^+ ion bombardment on SiO_2 with experimental data from several sources. As shown in Ref. 37, the computed etch yield is slightly larger than the experimentally measured yields over the range of energy considered, although there is considerable spread in experimental data as well. The computed yield does, however, capture the correct trend of SiO_2 sputter yield with ion energy and the etch threshold. The complexity of the underlying physical processes makes more thorough validation essential, although it is difficult at present given the scarcity of relevant experimental data that can be used for quantitative comparison. Without this direct validation against experiments, we consider the results presented here semiquantitative. The biggest source of uncertainty in our opinion is the fidelity of the pseudopotentials and the model in capturing low energy (<1 eV) processes.

III. RESULTS

We investigate the layer-by-layer etching of SiO_2 and Si in this article using low energy fluorocarbon and Ar^+ ions. These ions can, for example, be extracted from a high density plasma or equivalent source. Our goal is to examine the following sequence of processes:

(a)   the deposition of a thin fluorocarbon layer on the material surface using low energy CF_x^+ ions and

(b)   the removal of the top layer of the material using Ar^+ ions in a manner that only the amount of material commensurate with F on the surface is removed through reactive ion etching.

These steps are to be repeated until the desired depth has been etched. It is anticipated that more than one atomic layer will be etched during each step and the surface might become rough on an atomic scale. The use of a fluorocarbon passivation layer will not result in atomic layer etching *per se*, but will lead to the layer-by-layer etching of the material in which dimensions can be controlled on a nanometer scale.

We first focus on SiO_2. The SiO_2 test structure on which ion bombardment simulations are conducted is shown in Fig. 1(a). This is a perfect crystal of α quartz with dimensions $24.57 \times 25.53 \times 27.6$ Å^3. A thin fluorocarbon layer is grown on this test structure using 20 eV CF_2^+ or CF_3^+ ion bombardment at normal incidence. These ions can, for example, be extracted from plasmas based on C_2F_4 and C_2F_6, respectively. An adaptive time step is used during the simulations, and the initial location of the ion is chosen randomly above the sample. The time interval between subsequent simulations is 0.8 ps. During the first 0.25 ps of each ion impact, temperature control was turned off in the simulations. The temperature of the sample was controlled at 300 K for the remainder of the ion impact time. The test structure after 100 and 200 continuous impacts of 20 eV CF_2^+ ions is shown in Figs. 1(b) and 1(c), respectively. The number of F and C in the test structure as a function of the number of ion impacts is shown in Fig. 2. The fluorocarbon layer gradually grows
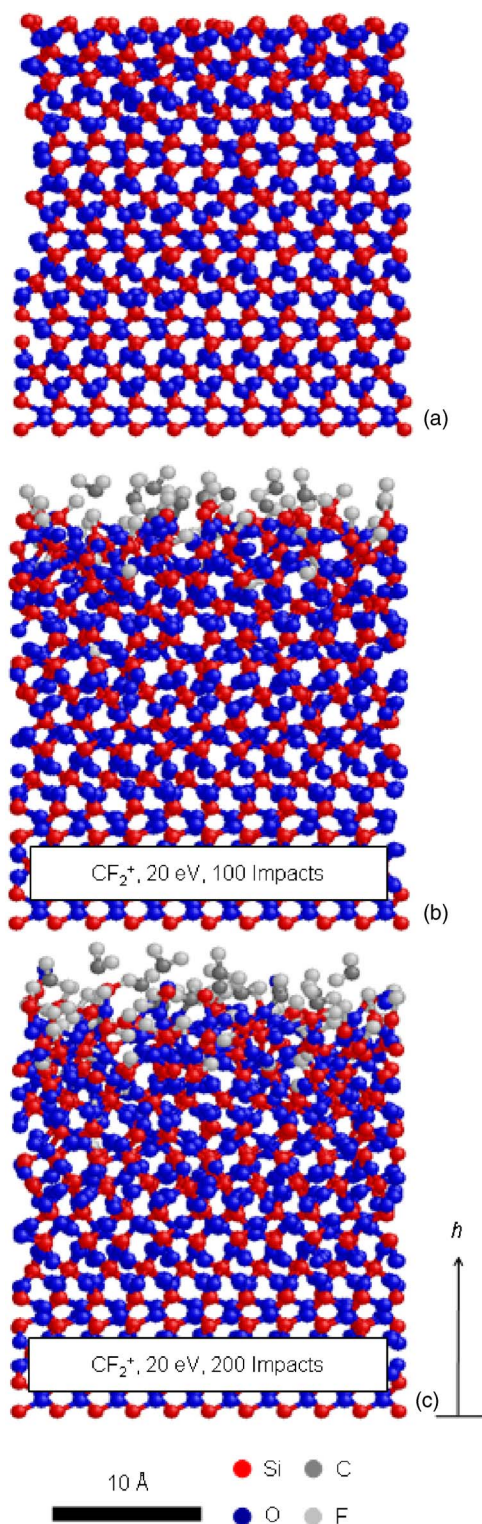
FIG. 1. (Color online) (a) Crystalline SiO_2 sample used for the molecular dynamics investigation in this article. (b) The SiO_2 sample after 100 impacts of 20 eV CF_2^+ ions. (c) The SiO_2 sample after 200 impacts of 20 eV CF_2^+ ions.

thicker and denser, and its composition and thickness eventually reach quasi-steady-state conditions. From the results in Fig. 2, it can be observed that both C and F concentrations saturate after about 250 ion impacts. The fluorocarbon is rich in F, i.e., F/C≫1. The F/C ratio is observed to decrease as ion energy is decreased, and this effect is later demonstrated
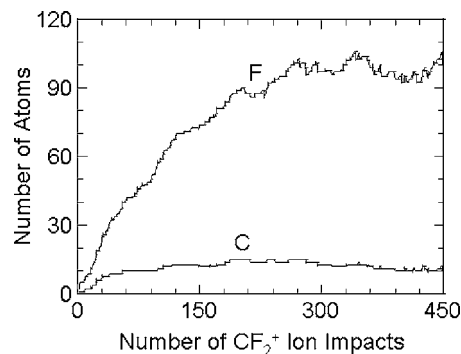

FIG. 2. F and C atoms in the SiO_2 sample as a function of the number of 20 eV CF_2^+ ion impacts.

for Si. C is sputtered with relative ease from the surface if incident ion energy is greater than 10 eV, which results in the F rich film. C sputters more easily compared to F as F–Si is stronger than the C–Si bond.[37]

We have plotted F concentration as a function of height h within the test structure for different numbers of CF_2^+ ion impacts in Fig. 3, where h has been measured with respect to structure bottom [Fig. 1(c)]. The passivation layer at the top is about 8 Å thick, and its thickness does not change significantly after 200 ion impacts. From the results in Fig. 1, the roughness of the fluorocarbon passivation film is less than 5 Å but the top 10 Å of the SiO_2 crystal is amorphized due to CF_2^+ ion bombardment. One can possibly reduce the thickness of the amorphization region by reducing ion energy, but we have not currently explored this scenario.

Figure 4 shows the SiO_2 test structure in Fig. 1(a) after bombardment with 20 eV CF_3^+ ions. The test structure is shown after 200 and 400 impacts. The corresponding number of F and C atoms in the test structure is plotted in Fig. 5 as a function of the number of ion impacts. Compared to CF_2^+ ions, it takes longer to reach steady-state conditions with CF_3^+ and the fluorocarbon passivation film has less C. At 20 eV, a large number of incident ions are found to "reflect" back as equivalent neutral without fragmentation or reaction. The proportion of reflected CF_3^+ ions is larger than CF_2^+ ions (for simulations described previously, Figs. 1–3) due to fewer C dangling bonds in CF_3^+ and the presence of more F in the near surface region which terminate the available bonds and make the particle unreactive. CF_3^+ ions therefore react less, and it takes longer for the fluorocarbon passivation
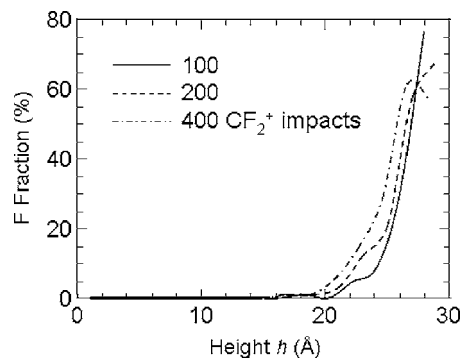

FIG. 3. Fluorine concentration in the sample as a function of sample height for different numbers of 20 eV CF_2^+ ion impacts.
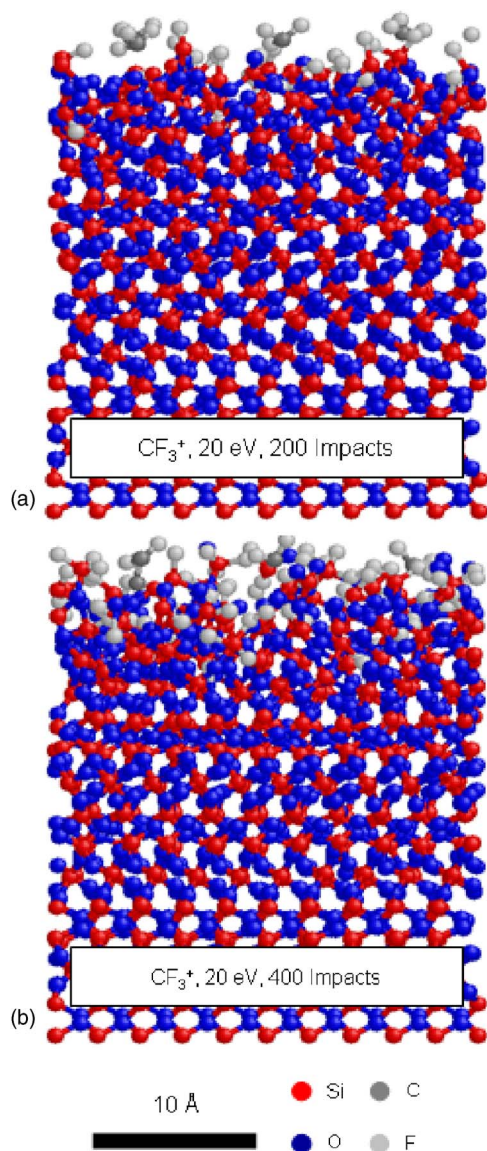
FIG. 4. (Color online) The SiO$_2$ sample after (a) 200 and (b) 400 impacts of 20 eV CF$_3^+$ ions.

film to reach steady state with CF$_3^+$ ions. The passivation film grown through CF$_3^+$ ion bombardment has less F compared to the film grown through CF$_2^+$ ion bombardment, and the F concentration profile shows that the passivation film is thinner if grown using CF$_3^+$ ions.
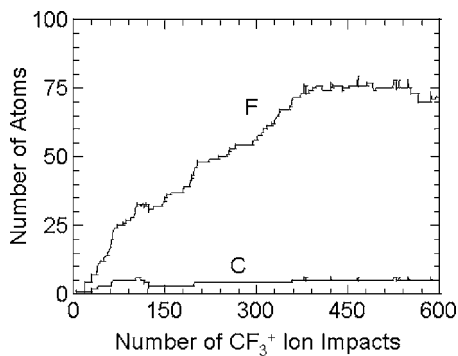

FIG. 5. F and C atoms in the SiO$_2$ sample as a function of the number of 20 eV CF$_3^+$ ion impacts.
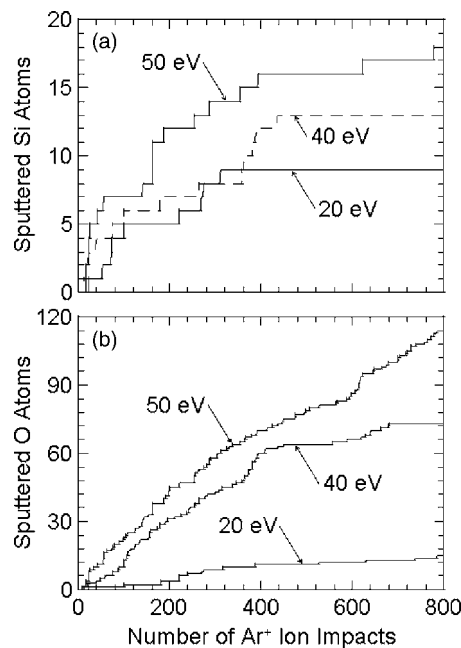

FIG. 6. Effect of Ar$^+$ ion energy on the number of Si and O atoms sputtered from the SiO$_2$ sample with a fluorocarbon overlayer grown using CF$_3^+$ ions (400 impacts).

To examine the second step of the layer-by-layer etch process, we bombarded the test structure in Fig. 4(b) with Ar$^+$ ions having energies between 20 and 50 eV. The fluorocarbon passivation layer on this test structure has been deposited using 20 eV CF$_3^+$ ions. For reference, the physical sputtering threshold for SiO$_2$ is about 50 eV.[37] The number of sputtered Si and O atoms is plotted in Fig. 6 as a function of the number of Ar$^+$ ion impacts. Si and O are etched from the material as part of a variety of clusters, where the term "cluster" is used here to collectively refer to sputtered atoms, molecules, radicals, or large atomic aggregates. Dominant clusters include SiF$_x$ (x=2,3), SiO$_x$F$_y$ (x=1,2; y=2,3,4), CO, and CO$_2$. Results in Fig. 6 include Si and O atoms in all clusters. It is found that, in the presence of F atoms on the surface, Si is initially etched for all Ar$^+$ ion energies considered. However, as the concentration of F atoms in the near surface region decreases, the sputtering of Si atoms ceases at 20 eV Ar$^+$ ion energy. The sputtering of Si atoms stops at 40 eV as well, although more Si atoms are removed from the surface. At 50 eV, Si continues to etch even after F concentration at the surface has been reduced although the etch rate decreases. In contrast to Si atoms, O atom ejection from the surface does not stop even up to 800 Ar$^+$ ion impacts, the maximum number of ion impacts we have examined. The rate of O loss, however, decreases after the initial stage of Ar$^+$ ion bombardment for ion energies below 40 eV. Each O atom is bound to two Si atoms in a crystalline SiO$_2$ lattice while Si atoms are attached to four O atoms. As Si–O bond energy is about 4.2eV, ~16.8 eV is needed to liberate a Si atom from the lattice. O atoms, on the other hand, only require ~8.4 eV to break free from the lattice. Because of this lower energy requirement, O atoms continue to exit the material at a slow pace even after Si sputtering has ceased. It is expected that the region near the surface will become deficient in O atoms before O etching stops.
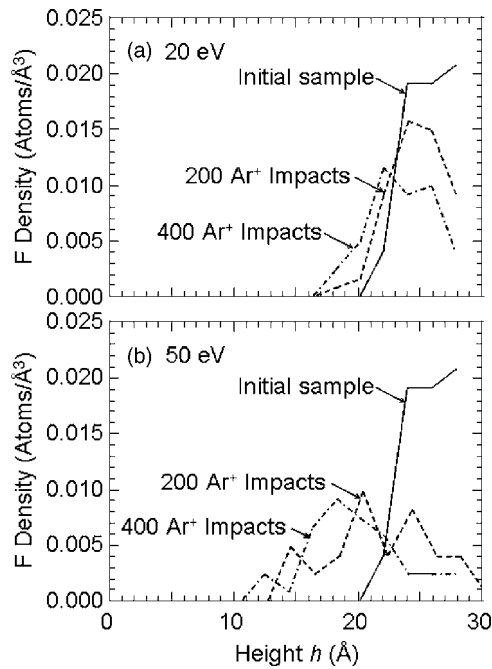
FIG. 7. Effect of Ar⁺ ion impact on F density in the SiO₂ sample with a fluorocarbon overlayer grown using CF_3^+ ions (400 impacts). Results have been plotted for (a) 20 eV and (b) 50 eV Ar⁺ ion energies.

As Ar⁺ ions continue to bombard the SiO₂ test structure with the fluorocarbon passivation layer, F atoms etch away Si atoms from the surface. In addition, F atoms are also pushed down into the bulk SiO₂ material, making them less accessible to the bombarding ions. We have shown the concentration of F atoms in the fluorocarbon passivated SiO₂ test structure in Fig. 7 at several stages during Ar⁺ ion bombardment. Results have been shown for 20 and 50 eV Ar⁺ ion energies. For both energies, F concentration decreases as the F atoms are removed through etching. At 20 eV, F atoms are not pushed far into the film by the bombarding atoms. However, it can be observed that F atom concentration becomes considerably broad through ion bombardment at 50 eV. MD is a computationally expensive technique, and it is difficult to follow the ion bombardment process for very long. It is expected that, as the F atoms are present in the test structure even after Si sputtering visibly stops at 20 eV [Fig. 6(a)], the F atoms will continue to etch Si either through reactive ion etching or through chemical means. We have currently not examined these long time scale processes.

Bombardment with Ar⁺ ions not only etches the top layer of SiO₂ but also amorphizes the remaining material and can potentially introduce surface roughness. We have shown the SiO₂ test structure after bombardment by 400 Ar⁺ ions of energies of 20 and 40 eV in Fig. 8. The initial sample had a fluorocarbon overlayer grown using CF_3^+ ions (400 impacts). Compared to the sample in Fig. 4(b), one can observe that Ar⁺ ion bombardment increases the thickness of the amorphized top layer and the amorphized region is thicker when Ar⁺ ions are more energetic. This is because more energetic Ar⁺ ions can penetrate deeper into the sample. Due to the small sample size, it is difficult to determine if surface roughness has changed due to Ar⁺ ion bombardment.
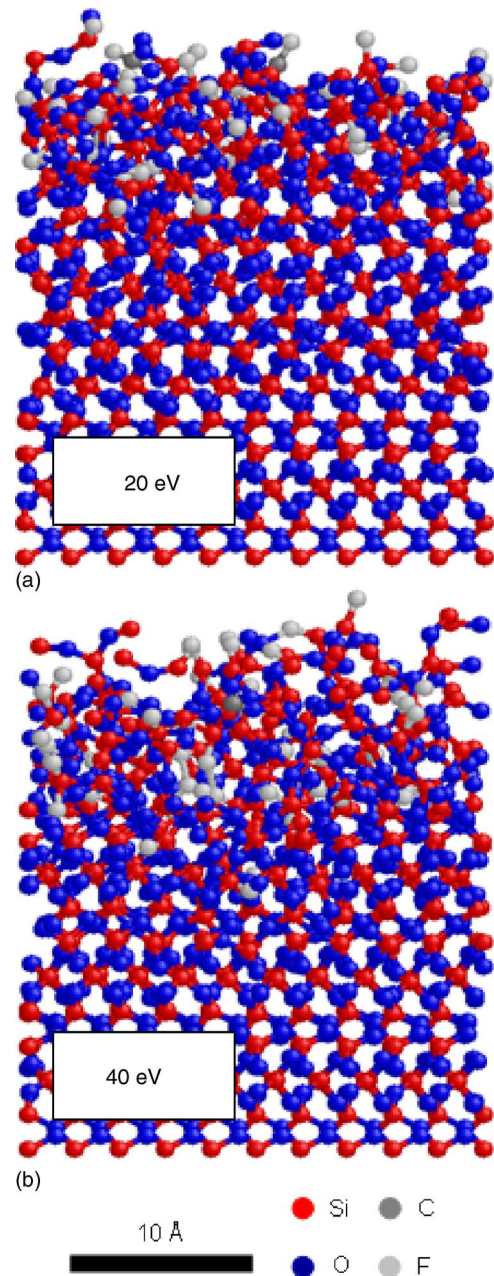
Similar to SiO₂, fluorocarbon species also form a thick

FIG. 8. (Color online) Side view of the SiO₂ sample after bombardment by 400 Ar⁺ ions of energies of (a) 20 eV and (b) 40 eV. This sample had initially a fluorocarbon overlayer grown using 20 eV CF_3^+ ions (400 impacts).

passivation layer on Si surface. It is therefore possible to use the layer-by-layer etch process described above for Si as well. We next examine the two steps of the layer-by-layer etching process (fluorocarbon passivation layer deposition and Ar⁺ ion etching) for Si. The initial crystalline Si test structure is shown in Fig. 9(a), and it is 27.17×27.17 ×38.04 Å³ in size. Before any bombardment took place on this test structure, it was equilibrated at 300 K. Following equilibration, the test structure was bombarded with CF_2^+ ions with energies of 10, 20, and 30 eV. During the first 0.25 ps of each ion impact simulation, thermal control was turned off. For the remainder of the 0.8 ps ion impact time period, the external thermal bath was set at 300 K. The resulting samples in quasi-steady-state condition for three ion
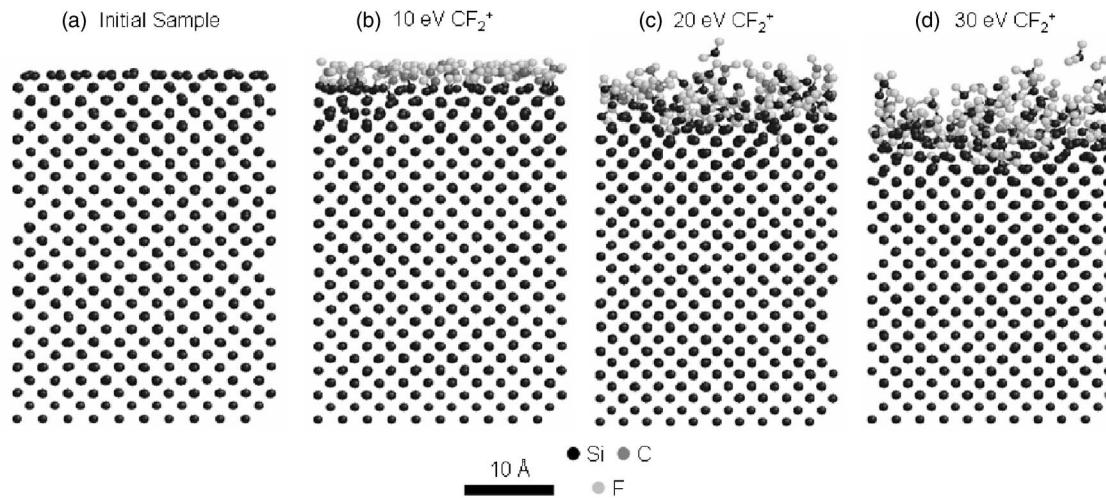
FIG. 9. (a) Initial Si sample. The sample after bombardment with CF_2^+ ions of energies of (a) 10 eV, (b) 20 eV, and (c) 30 eV.

energies are shown in Figs. 9(b)–9(d). At 10 eV ion energy, the underlying Si lattice is barely disturbed and a 4–5 Å thick fluorocarbon passivation layer is grown on top of Si. The fluorocarbon passivation layer thickens as CF_2^+ ion energy is increased, and F and C atoms also penetrate the underlying Si. By comparing the samples in Fig. 9, it can be observed that some amount of Si etching also occurs at 30 eV. It is therefore inferred that a fluorocarbon passivation layer can be grown on Si for layer-by-layer etching if ion energy is kept below 30 eV. The passivation layer is about 8 Å thick at 20 eV CF_2^+ ion energy.

We have shown the number of F and C atoms in the test structure in Fig. 10 as a function of the number of CF_2^+ ion impacts. Results have been plotted for 10 and 20 eV CF_2^+ ion bombardments. F and C reach quasi-steady-state condition for all ion energies considered after about 450 CF_2^+ ion

impacts. The film contains considerably more C at 10 eV than at higher energies, and the fluorocarbon layer is F rich at higher energies.

The thickness of passivation layer can be extracted from the F density plots shown in Fig. 11. These results have been plotted for 10 and 30 eV CF_2^+ ion energies. At 10 eV, F concentration in the film increases as more CF_2^+ ions bombard the sample. The F concentration for 600 ion impact is close to quasi-steady-state and the fluorocarbon film is about 5 Å thick. The F containing passivation layer is much broader at 30 eV. From the density profiles at 300 and 600 ion impacts [Fig. 11(b)], it can be observed that the F layer is moving downwards, which is due to the etching of the underlying Si.

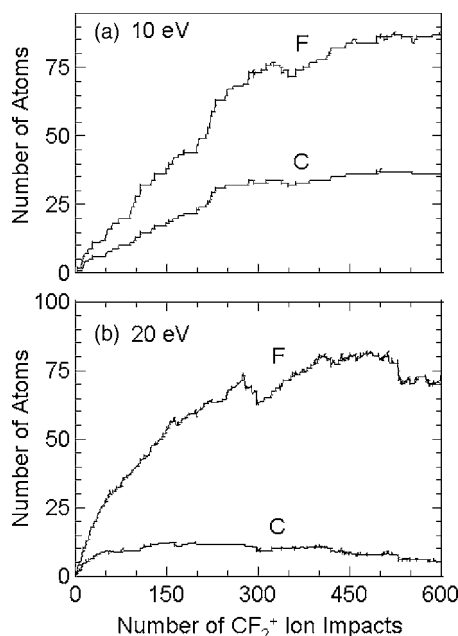The second step of the atomic layer-by-layer etch pro-

FIG. 10. Number of F and C atoms in the Si sample after bombardment with CF_2^+ ions. Results have been plotted for (a) 10 eV and (b) 20 eV ion energies.
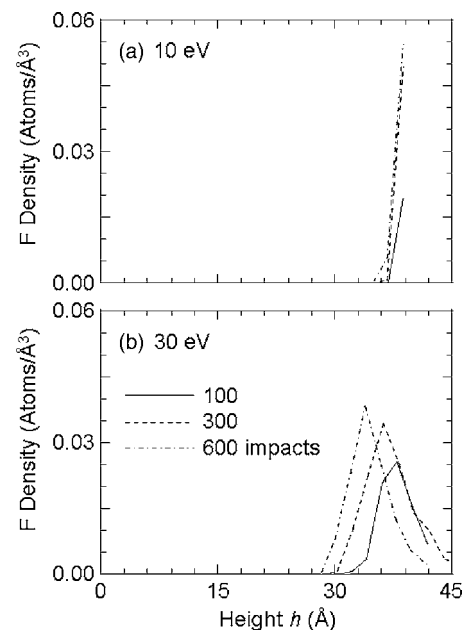

FIG. 11. F density as a function of sample height in the Si sample with the fluorocarbon overlayer. Results have been plotted for 100, 300, and 600 CF_2^+ ion impacts on the initial crystalline sample. CF_2^+ ion energies are (a) 10 and (b) 30 eV.
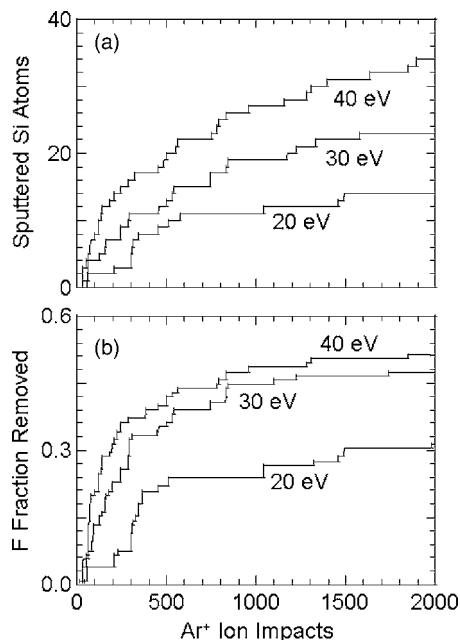
FIG. 12. (a) Number of Si atoms that are sputtered from the Si sample with the fluorocarbon overlayer (10 eV CF_2^+, 300 impacts) as Ar^+ ions of different energies are bombarded on it. (b) Fraction of initial F left in the sample as Ar^+ ions of different energies are bombarded on the Si sample with the fluorocarbon overlayer (10 eV CF_2^+, 300 impacts).
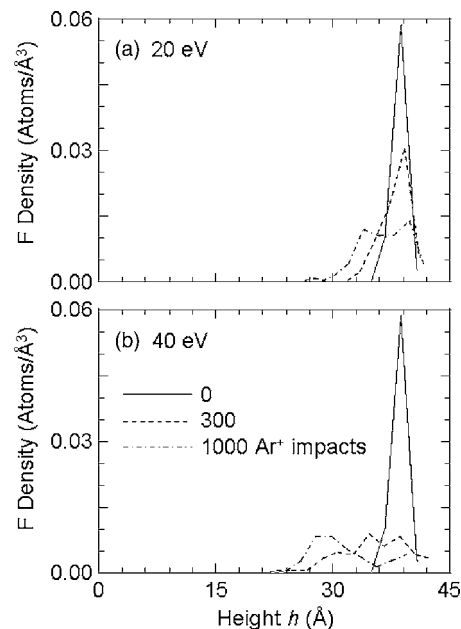

FIG. 13. F density as a function of sample height in the Si sample with the fluorocarbon overlayer (10 eV CF_2^+, 300 impacts). Results have been plotted for the initial sample and after 300 and 600 Ar^+ ion impacts. Ar^+ ion energies are (a) 20 and (b) 40 eV.

cess is the Ar^+ ion etching of the fluorocarbon passivated Si sample. We used the test structure in Fig. 9(b) for this purpose, which has been grown using 10 eV CF_2^+ ions. This test structure was continuously bombarded with Ar^+ ions with energies of 20–40 eV. The number of sputtered Si atoms and fraction of initial F removed from the sample are shown in Fig. 12 as a function of the number of Ar^+ ion impacts. Results for 20, 30, and 40 eV ion energies have been plotted. These results show that Si is initially etched from the sample and the number of F atoms in the sample also decreases. The rate of Si or F loss increases with ion energy. After the initial stage of etching, Si loss virtually stops at 20 eV. As explained earlier in the context of SiO_2, there is still considerable amount of F left in the sample so the slow loss of Si (in combination with F) cannot be precluded. At 30 eV, Si sputtering has slowed down by the end of our simulation, although it has not completely stopped. The rate of Si loss is substantial at 40 eV even up to the end of the simulation (1000 Ar^+ ion impacts). Ar^+ ion energies below 30 eV therefore appear well suited for the layer-by-layer etching of Si.

We have shown the concentration of F within the film at several stages during the Ar^+ ion bombardment process in Fig. 13. Results for 20 and 40 eV have been plotted. At 20 eV, one can observe that F is lost from the sample as more Ar^+ ions are bombarded on the test structure. F atoms are also pushed slightly downwards into the test structure. The same effects are observed at 40 eV as well, although F concentration is broader at 40 eV and F is spread over ∼18 Å by the end of the simulation.

Similar to SiO_2, bombardment with Ar^+ ions is expected to amorphize the top layers of the remaining Si and introduce surface roughness. We have shown the Si test structure after bombardment by 1000 Ar^+ ions of energies of 20 and 40 eV

in Fig. 14. The initial sample had a fluorocarbon overlayer grown using 10 eV CF_2^+ ions (300 impacts). Compared to the sample in Fig. 9(b), one can observe that Ar^+ ion bombardment increases the thickness of the amorphized top layer and the amorphized region is thicker when Ar^+ ions are more energetic. This is because more energetic Ar^+ ions can penetrate deeper into the sample.

IV. CONCLUSIONS

A MD model is used to understand layer-by-layer etching of Si and SiO_2 using fluorocarbon and Ar^+ ions in this article. Both the passivation and etching steps are examined. In these etch processes, a nanometer-scale fluorocarbon passivation layer is grown on the material's surface using low energy CF_x^+ ions or radicals. The top layers of the material are then reactive ion etched by Ar^+ ions utilizing the fluorocarbon already present on the material surface. By repeating these two steps, Si or SiO_2 can be etched with nanometer-scale precision and the etch rate is considerably faster than what traditional atomic layer etching techniques provide. The modeling results show that fluorocarbon passivation films can be grown in a self-limiting manner on both Si and SiO_2 using low energy CF_2^+ and CF_3^+ ions. The fluorocarbon passivation layer is a few angstroms thick, and its thickness increases with the fluorocarbon ion's energy. Increasing the ion energy, however, amorphizes the top atomic layers of the material. In addition, the fluorocarbon film becomes F rich with increasing ion energy. Simulations of fluorocarbon passivated SiO_2 surface show that Ar^+ ions with energy below 50 eV etch Si (within SiO_2) in a self-limiting manner. Si etching stops once F in the fluorocarbon passivation layer is exhausted or it is pushed too deep into the substrate. On the other hand, oxygen (within SiO_2) is more easily sputtered from the material surface than Si, and the top layers of SiO_2
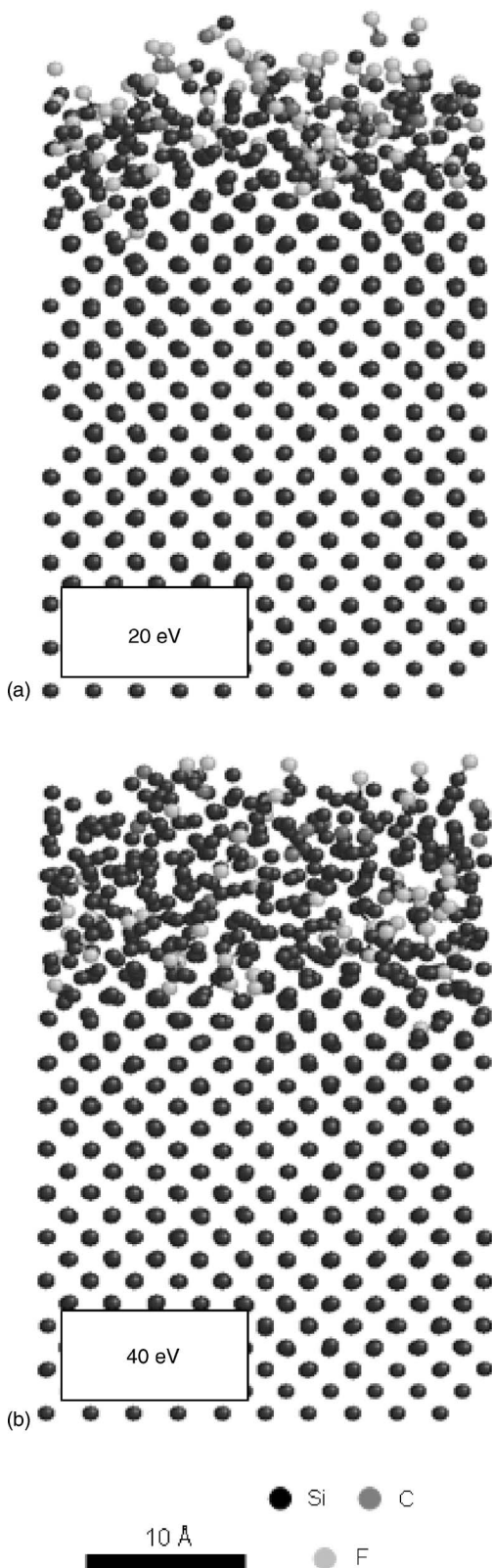
FIG. 14. Si sample after bombardment by 1000 Ar$^+$ ions with energies of (a) 20 and (b) 40 eV. The initial Si sample had a fluorocarbon overlayer grown using 10 eV CF$_2^+$ ions (300 impacts).

The layer-by-layer etching of Si or dielectrics is a complex physical phenomenon. Our investigation is an attempt to theoretically understand the intricacies of the relevant surface processes during etching and, by necessity, only addresses a subset of the complete problem. For example, as the pseudopotentials are not expected to adequately capture low energy chemical processes, we have grown the fluorocarbon passivation layers through fluorocarbon ion bombardment with ion energies above 10 eV. We are currently attempting to improve the pseudopotentials to better capture chemical effects, which will allow the treatment of fluorocarbon passivation film growth using even lower energy ions or neutral radicals. The results presented in this article are also specific to the crystalline test structures for SiO$_2$ [Fig. 1(a)] and Si [Fig. 9(a)]. It is unclear how well the observed trends will translate to amorphous films.

are expected to become deficient in O during the Ar$^+$ ion bombardment step. Ar$^+$ ion etching of fluorocarbon passivated Si also appears to be self-limiting below 30 eV ion energy, and etching stops once F on the material surface is either consumed or becomes inaccessible.

[1] M.-H. Cho *et al.*, Appl. Phys. Lett. **81**, 472 (2002).
[2] S. M. Rossnagel, A. Sherman, and F. Turner, J. Vac. Sci. Technol. B **18**, 2016 (2000).
[3] H. Kim, J. Vac. Sci. Technol. B **21**, 2231 (2003).
[4] S. D. Athavale and D. J. Economou, J. Vac. Sci. Technol. A **13**, 966 (1995).
[5] T. Matsuura, J. Murota, Y. Sawada, and T. Ohmi, Appl. Phys. Lett. **63**, 2803 (1993).
[6] T. Meguro, M. Ishii, T. Sugano, K. Gamo, and Y. Aoyagi, Appl. Surf. Sci. **82–83**, 193 (1994).
[7] K. Ikeda, S. Imai, and M. Matsumara, Appl. Surf. Sci. **112**, 87 (1997).
[8] W. T. Tsang, T. H. Chiu, and R. M. Kapre, Appl. Phys. Lett. **63**, 3500 (1993).
[9] T. Matsuura, Y. Honda, and J. Murota, Appl. Phys. Lett. **74**, 3573 (1999).
[10] T. Sugiyama, T. Matsuura, and J. Murota, Appl. Surf. Sci. **187**, 187 (1997).
[11] N. Otsuka, J. Nishizawa, Y. Oyama, H. Kikuchi, and K. Suto, J. Electrochem. Soc. **146**, 547 (1999).
[12] S. D. Park, D. H. Lee, and G. Y. Geom, Electrochem. Solid-State Lett. **8**, C106 (2005).
[13] S. Matsui, M. Baba, and A. Satoh, Nanotechnology **3**, 156 (1992).
[14] H. Sakaue, S. Iseda, K. Asami, J. Yamamoto, M. Hirose, and Y. Horiike, Jpn. J. Appl. Phys., Part 1 **29**, 2648 (1990).
[15] S. D. Park, K.-S. Min, B.-Y. Yoon, D.-H. Lee, and G.-Y. Geom, Jpn. J. Appl. Phys., Part 1 **44**, 389 (2005).
[16] Y. Horiike *et al.*, J. Vac. Sci. Technol. A **8**, 1844 (1990).
[17] Y. Horiike *et al.*, J. Vac. Sci. Technol. A **8**, 1844 (1990).
[18] S. D. Athavale and D. J. Economou, J. Vac. Sci. Technol. B **14**, 3702 (1996).
[19] T. Matsuura, T. Sugiyama, and J. Murota, Surf. Sci. **402**, 202 (1998).
[20] J. Yamamoto, T. Kawasaki, H. Sakaue, S. Shingubara, and Y. Horiike, Thin Solid Films **225**, 124 (1993).
[21] M. Matsui, T. Tatsumi, and M. Sekine, J. Vac. Sci. Technol. A **19**, 1282 (2001).
[22] M. Matsui, T. Tatsumi, and M. Sekine, J. Vac. Sci. Technol. A **19**, 2089 (2001).
[23] M. Schaepkens, G. S. Oehrlein, C. Hedlund, L. B. Jonsson, and H. Blom, J. Vac. Sci. Technol. A **16**, 3281 (1998).
[24] M. Schaepkens, T. E. F. M. Standaert, N. R. Rueger, P. G. M. Sebel, G. S. Oehrlein, and J. M. Cook, J. Vac. Sci. Technol. A **17**, 26 (1999).
[25] N. R. Rueger, M. F. Doemling, M. Schaepkens, J. J. Beulens, T. E. F. M. Standaert, and G. S. Oehrlein, J. Vac. Sci. Technol. A **17**, 2492 (1999).
[26] X. Li, X. Hua, L. Ling, G. S. Oehrlein, M. Barela, and H. M. Anderson, J. Vac. Sci. Technol. A **20**, 2052 (2002).
[27] M. Inayoshi, M. Ito, M. Hori, T. Goto, and M. Hiramatsu, J. Vac. Sci. Technol. A **16**, 233 (1998).
[28] K. Takahashi, M. Hori, and T. Goto, J. Vac. Sci. Technol. A **14**, 2011 (1996).
[29] M. Chander, Y. Z. Li, J. C. Patrin, and J. H. Weaver, Phys. Rev. B **47**, 13035 (1993).
[30] C. M. Aldao and J. H. Weaver, Prog. Surf. Sci. **68**, 189 (2001).
[31] M. Chander, D. A. Goetsch, C. M. Aldao, and J. H. Weaver, Phys. Rev. Lett. **74**, 2014 (1995).

[32]C. F. Abrams and D. B. Graves, J. Appl. Phys. **86**, 5938 (1999).
[33]C. F. Abrams and D. B. Graves, J. Vac. Sci. Technol. A **18**, 411 (2000).
[34]C. F. Abrams and D. B. Graves, J. Appl. Phys. **88**, 3734 (2000).
[35]C. F. Abrams and D. B. Graves, J. Vac. Sci. Technol. A **19**, 175 (2001).
[36]H. Ohta and S. Hamaguchi, J. Vac. Sci. Technol. A **19**, 2373 (2001).
[37]V. V. Smirnov, A. V. Stengach, K. G. Gaynullin, V. A. Pavlovsky, S. Rauf, P. J. Stout, and P. L. G. Ventzek, J. Appl. Phys. **97**, 093302 (2005).
[38]V. V. Smirnov, A. V. Stengach, K. G. Gaynullin, V. A. Pavlovsky, S. Rauf, P. J. Stout, and P. L. G. Ventzek, J. Appl. Phys. **97**, 093303 (2005).
[39]M. J. Frisch *et al.*, GAUSSIAN98, Revision A.9, Gaussian, Inc., Pittsburgh, PA, 1998.
[40]M. P. Allen and D. J. Tildesley, *Computer Simulation of Liquids* (Clarendon, Oxford, 1994).
[41]H. J. C. Berendsen, J. P. M. Postma, W. F. van Gunsteren, A. DiNola, and J. R. Yaak, J. Chem. Phys. **81**, 3684 (1984).

28 April 2025 14:41:11